HYDROTREATMENT EFFECTS ON WILSONVILLE COAL LIQUIDS; COMPUTER-ASSISTED EVALUATION OF MULTISOURCE ANALYTICAL DATA

Koli Taghizadeh, Rita Hardy, Robert Keogh, Jack Goodman, Burt Davis
Kentucky Energy Cabinet Laboratory, Lexington, KY 40512

Henk L.C. Meuzelaar
University of Utah, Biomaterials Profiling Center
Salt Lake City, Utah 84108

INTRODUCTION

As reported earlier (1), monitoring time-dependent changes in Wilsonville coal-derived liquid (CDL) streams by means of computer-assisted direct mass spectrometry (MS) techniques enables detection of process related trends in the relative concentration of CDL components. Notwithstanding the potentially high information yield of this MS procedure, additional data is required for unambiguous identification and interpretation of some of the more complex components or trends. In fact, the CDL's produced by the Wilsonville pilot plant are routinely analyzed by an extensive array of conventional tests, including elemental analysis and solubility classes, as well as by advanced chromatographic and/or spectroscopic techniques, e.g., proton nuclear magnetic resonance spectroscopy (NMR) and carbon-13 NMR.

Unfortunately, the sheer volume of the data produced by this broad array of tests during a 2 to 3 month run makes it very difficult to discern some of the more interesting trends and effects. In the experiments reported here computerized multivariate analysis techniques such as factor, discriminant and canonical correlation analysis, were used to remove redundant data or experimental noise and to highlight relevant components and trends.

EXPERIMENTAL

A schematic flow diagram of the Wilsonville Advanced Coal Liquefaction facility in the Integrated Two-Stage Liquefaction (ITSL) mode is shown in Figure 1. The feed to the second stage hydrotreater is a mixture of thermal distillate (450^{o}F+) and Critical Solvent De-ashed Thermal Residue (CSD TR). The hydrotreater "atmospheric flashed bottoms" stream is recycled to the first stage dissolver. The temperature/time profile of the hydrotreater as well as a seven day average of the difference (ΔT) between the outlet and inlet temperature of dissolver are shown in Figure 2. The hydrotreater temperature was increased in 10^{o}F increments from 720^{o}F to 740^{o}F as the catalyst aged. However, as shown in Figure 2, several times during the run, operator responses to technical problems caused the actual hydrotreater temperature to be much lower than the set temperature. It is intended that the dissolver temperature be controlled primarily by the temperature of the preheated coal slurry, which flows from a preheater into the dissolver.

The data presented here were generated for samples collected during run No. 244 at the Wilsonville pilot plant when they were processing an Illinois No. 6 coal from a Burning Star mine. The average composition of the coal was: proximate analysis - VM 36%, FC 50%, moist. 4%, ash 10%; ultimate analysis - C 68.2%, H 4.5%, N 1.2%, S 3.3, mineral matter 10.6%, O (diff.) 12.2%. The sampling points for both hydrotreater feed and hydrotreater product (atmospheric flashed bottoms) samples are shown in Figure 1 and the days on which samples were collected are indicated in Figure 2. For consistency with earlier work (1), that numbering system was retained; unfortunately, the NMR and conventional data were not available for sample nos. 2, 3, 4, 12, 13 and 14. Therefore these samples were omitted from this data set.

Elemental carbon, hydrogen and nitrogen values were obtained using a LECO CHN-600 analyzer (2). Direct oxygen determinations were obtained by a modified Unterazucher method (3), and sulfur determinations were made on a LECO SC-132 instrument (4). The solubility class (oils, asphaltenes, preasphaltenes) and phenols determinations were described in detail elsewhere (5,6). Vacuum distillations utilized a modified ASTM D-1160 apparatus that was maintained at approximately 0.1 mmHg during the distillation. Following standard practice, the distillation was considered to be complete when cracking became noticeable.

Proton NMR samples were prepared by diluting approximately 0.25 g of the CDL with 0.25 ml of $CDCl_3$ which was doped with 1 wt. % TMS (tetramethyl silane). Spectra were recorded on a Varian EM-390 instrument. A minimum of two integrations were recorded for the proton regions determined. The proton spectra were divided into seven regions which correspond to different proton type resonances (7). Samples for carbon 13-NMR were prepared by diluting 1.5 g of the CDL with 1.0 ml of $CDCl_3$. Five mg of $Cr[acac]_3$ was added as a relaxation agent. Spectra were recorded with a Varian FT-80 spectrometer over a 4000 Hz spectral window at 20 MHz. Integrals were obtained in duplicate. The carbon 13-NMR spectra were divided into an aliphatic (0-50 ppm) and an aromatic region (100-200 ppm) (8).

Solutions for low voltage MS were prepared as follows: about 2 mg of each CDL were weighed and dissolved in 1 ml of a 1:1 benzene:methanol mixture. Solutions were stored at -10 ^{o}C prior to analysis. Low voltage MS were obtained using an Extranuclear 5000-1 quadrupole system under the following conditions: temperature rise time 5.5 s, equilibrium temperature 610 ^{o}C, total heating time 10 s, electron energy setting 12 eV, mass range scanned m/z 20-260, scanning rate 1000 amu/s, total scan time 20 s. Each sample was analyzed in triplicate and the resulting spectra were normalized using the SIGMA program package (9).

Data analysis was performed using factor analysis and canonical correlation analysis procedures, described elsewhere in more detail (10,11 and 12). Canonical correlation analysis was used to compare two data sets, e.g., on the basis of factor scores. The canonical correlation technique constructs sets of linear combinations of the variables in the two data sets in such a way that the first linear combination (canonical variate function) for the first data set and the first linear combination of the second data set show maximum correlation. The second set of linear combinations describes the maximum correlation remaining in the data set and so on.

RESULTS AND DISCUSSION

Figure 3 shows the averaged low voltage mass spectra of the hydrotreater feed and hydrotreater product (flashed bottoms). The hydrotreater feed spectrum shows relatively prominent peak series at m/z 168, 182, 196, 210 and 224, tentatively identified as acenapthenes and/or biphenyls with various of alkylsubstitution. The hydrotreater product spectrum shows major peak series at m/z 172, 186, 200, 214, and 228; these are believed to represent hydroaromatic hydrocarbons such as octahydrophenanthrenes and/or hexahydrofluorenes with possible contributions from tetrahydroacenaphthenes.

Other homologous ion series at m/z 212, 226, 240, 254 in the hydrotreated product spectrum obviously represent decahydropyrenes and perhaps decahydrofluoranthenes. Although there is no direct way to identify the various mass peaks in Figure 3, all major compound series were tentatively identified by GC/MS as well as MS/MS analysis of selected samples and compounds as well as by comparisons with GC/MS literature data on Wilsonville CDL's (13,14). Close scrutiny of Figure 3 may raise the question why the main compound series observed in the hydrotreater product does not correspond directly to the main compound series in the hydrotreater feed? An obvious answer is that the hydroaromatic compounds formed during hydrotreatment are

substantially more volatile than the corresponding aromatic parent compound series. Consequently, many of these low boiling volatiles are removed in the atmospheric distillation overhead fraction (see Figure 1).

A second aspect which should be pointed out here is that the spectra in Figure 3 represent only the CDL components which were able to reach the ion source without preheating the MS inlet system. Consequently, compounds with about 5-rings and higher are not included in Figure 3. However, as established in a separate series of experiments (1) involving preheating of the MS inlet as well as comparisons with Field Ionization MS data obtained at SRI, differences seen in Figure 3 are quite characteristic and representative of the overall changes observed as a result of hydrotreatment even if these higher components had been volatilized. In other words, the changes observed for the 2-4 ring systems in Figure 3 were qualitatively similar to those observed in higher condensed compound series.

To enable more systematic comparisons among the spectra of all 14 samples, the low voltage MS data were subjected to factor analysis. Figure 4 shows the factor score plot of the first two factors, together explaining 74% of the total variance in the data. The hydrotreater feed (categories 1-10) and hydrotreater product (categories 11-20) samples form two distinct clusters. In fact, Factor I and Factor II, with 64.4% and 9.6% of total variance respectively, appear to reveal two major trends in the data set; namely a hydrotreatment effect (Factor I) and a time + temperature effect (Factor II, compare with the time + temperature trend in Figure 2). Factors I and II explained 74% of the total variance in the data whereas the remaining 26% was largely explained by factors 3-10, none of which revealed significant components or trends.

Conventional coal liquid characterization data as well as ^{1}H and ^{13}C NMR data obtained for both sets of samples are shown in Table I. The effects of hydrotreatment are immediately apparent upon inspection of many of the parameters in Table I. However, neither the time + temperature trend, observed in the low voltage MS data nor any of the other trends which might be present are readily discernible by visual examination of the multidimensional information in Table I. Consequently, multivariate statistical analysis techniques such as factor analysis, are needed to reduce the data and reveal the main underlying trends.

To obtain a better insight into the components and trends described by the NMR and conventional data, factor analysis was performed on this data set as well. Eight factors with eigenvalues >1.0, together describing a total variance of 98.6% were obtained. The score plot of the first two factors is shown in Figure 5 with Factor I (57.4%) and Factor II (13.6%) revealing the hydrotreatment effect and time + temperature effect respectively. Again, the remaining factors (27.6%) did not reveal any clear trends or components. Encouraged by the obvious similarities between the information provided by Figures 4 and 5, we determined the degree of overlap between the two data sets by means of canonical correlation analysis.

Two major canonical correlation functions were found, CVI (can. corr. = 0.998) and CVII (can. corr. = 0.946). The integrated score plot of both data sets is shown in Figure 6. To reduce the complexity of the low voltage MS data, the average of each triplicate analysis was plotted. As expected, the same two important trends were observed with CVI showing the effect of hydrotreatment and CVII describing a combined time + temperature effect.

Figure 7 shows the absolute difference between the CVI scores of hydrotreated feed and hydrotreated products of low voltage MS and conventional and NMR data; this enables a more direct evaluation of the efficiency of the hydrotreatment process to be made. Apparently, the differences between the composition of the hydrotreater

feed and the hydrotreater product sample become somewhat less pronounced towards the end of the run, indicating a loss of hydrotreatment efficiency with time.

Finally, Figures 8 and 9 allow a more detailed chemical evaluation of the trends and components represented by CVI and CVII. The mathematically extracted mass spectra of CVI (hydrotreatment effect) and CVII (time + temperature effect) are shown in Figure 8. The positive components of the spectrum Figure 8a, representative of the hydrotreater feed, show prominent acenaphthene and/or biphenyl series at m/z 168, 182, 196, 210, and 224 (compare with Figure 3a) as well as naphthalene series at m/z 142, 156, 170, 184, and 198. The negative components show dominant hydroaromatic ion series at m/z 172, 186, 200, 214, and 228 as well as at m/z 212, 226, and 240 (also observed in Figure 3b).

Interpretation of the spectrum of the second canonical variate function in Figure 8b is less straightforward. Obviously, we are looking at a shift in the average molecular weight of the vacuum distillate fraction that is seen by the mass spectrometer. As discussed above, the upper limit of the vacuum distillate range is primarily determined by the inlet temperature of the mass spectrometer. Conversely, the lower limit of the distillation range must be primarily determined by the cut-off point of the atmospheric distillation following hydrotreatment. This cut-off point is likely to reflect the steadily increasing hydrotreater temperature shown in Figure 2. Consequently, the early samples tend to be richer in low MW components than the later samples obtained at higher hydrotreater temperatures. This appears to be reflected in the trend shown in Figure 8b. Whether Figure 8b also reflects the effect of catalyst aging, e.g. in the form of changes in qualitative composition is hard to decide due to the close correlation between time and temperature in the overall experimental design shown in Figure 2. Moreover, minor but definite changes in overall coal quality, e.g., as a result of storage and/or variations in mine output, could also have contributed to the observed trends, thereby further complicating attempts at unambiguous chemical interpretation. Obviously, if these effects are to be distinguished in future studies, the experimental design of the process conditions will need to be aimed at decoupling the effects of catalyst aging, reactor temperatures, distillation conditions and changes in feed coal composition.

The loadings (correlation coefficients) of the NMR and conventional variables on the first canonical variate function are shown in Figure 9a. Heteroatomic concentrations (N, S, O), asphaltene and benzene insolubles as well as the relative concentration of all condensed and noncondensed aromatic protons and aromatic carbon are higher in the hydrotreater feed than in the product samples. Conversely, %C, %H, oil yield, relative concentration of alkyl and cyclic protons (H-NMR) and aliphatic carbons (carbon 13-NMR) are, as expected, higher in the hydrotreater product (flashed bottoms).

Loadings of NMR and conventional data on CVII (Figure 9b) show that hydrotreater temperature (T), dissolver temperature (ΔT) and time (t) show a strong, positive correlation with CVII (negative portion). With increasing time and temperature, more hydrogen is present in the nondistillate fraction which could reflect decreased catalyst efficiency; that is, the hydrocracking activity decreases relative to the hydrogenation activity. Moreover, heteroatoms such as N and S are not removed as efficiently in the later days of the run. The fact that %O appears to be higher in the early days may well be due to phenols at m/z 136, 150, 164 or a pseduocorrelation caused by the normalization of %C, H, N, O to 100%. Also distillate yields are higher in early days, whereas the nondistillate portion increases in later days. ^{1}H-NMR data show higher alkyl beta and gamma protons in early days. The low voltage MS data in Figure 8b indicate that this might be due to the presence of highly substituted tetralins and phenols. Conversely, the ^{1}H-NMR data show that the relative concentration of cyclic alphas and some type of cyclic beta hydrogen increases in later days; the higher hydroaromatics in low

voltage MS (Figure 8b) could account for this. Overall, the time + temperature trend represented by CVII indicates a loss of catalyst efficiency accompanied by decreased distillate yield, increased aromaticity and ring condensation and a substantial increase in hydrogen in the nondistillate fraction.

A speculative interpretation of the latter observation has catalyst aging producing a more pronounced loss of bond cleavage activity than of hydrogenation efficiency, thus resulting in the formation of alicyclic structures which remain in the increasingly larger nondistillate fraction. Alternatively, one might hypothesize that a loss of efficiency in capping newly formed radicals leads to an increased condensation through regressive reactions.

ACKNOWLEDGEMENTS

This work was supported by the Commonwealth of Kentucky, Kentucky Energy Cabinet and DOE Contract No. DEFC22-85PC80009 as part of the Consortium for Fossil Fuel Liquefaction Science (administrated by the University of Kentucky). Dr. W. Windig and Mrs. M. Van are acknowledged for invaluable discussion in data analysis and manuscript preparation. We also acknowledge the superior cooperation of the staff of the Wilsonville Alabama pilot plant.

REFERENCES

1. Taghizadeh, K., Davis, B., Meuzelaar, H.L.C., 35th Annual Conference on Mass Spectrometry and Allied Topics., May (1987).
2. Leco Corp., CHN-600 Instrument Manual No. 200-340 (1983).
3. Unterzaucher, J., Analyst., 77, 584 (1952).
4. Leco Corp., SC-132 Manual 200-170 (1980).
5. Schultz, H., Mima, M.J., Prep. Pap., Am. Chem. Soc. Div. Fuel Chem., 23, (2)768, (1978).
6. Davis, B., Thomas, G., Sagues, A., Jewitt, C., Baumert, K., IMMR 80/053, April (1980).
7. Burke, F.P., Winschel, R.A., Pochapshky, T.C., U.S. DOE Contract DE-AC05-79ET-14503, Final Report, FE-14503-3., November (1983).
8. Levy, G.C., Nelson, G.L., Carbon-13 Nuclear Magnetic Resonance for Organic Chemists, John Wiley and Sons., New York (1972).
9. Windig, W., Meuzelaar, H.L.C., 34th Annual Conference on Mass Spectrometry and Allied Topics., 64, (1986).
10. Windig, W., Meuzelaar, H.L.C., Anal. Chem. 56, 2297, (1984).
11. Windig, W., Meuzelaar, H.L.C., Haws, B.A., Campbell, W.F., Asay, K.H., Anal. Appl. Pyrolysis 5, 183, (1983).
12. Halma, G., Van Dam, D., Haverkamp, J., Windig, W., Meuzelaar, H.L.C, J. Anal. Appl. Pyrolysis., 7, 167, (1984).
13. Wozniak, T.J., Hites, R.A., Anal. Chem. 57, 1320, (1985).
14. Winschel, R.A., Burke, F.P., Proceedings 8th Annual EPRI Contractors Conference on Coal Liquefaction, (1983).

TABLE I
AVERAGED NMR AND CONVENTIONAL CHARACTERIZATION DATA FOR HYDROTREATER FEED AND HYDROTREATER PRODUCT SAMPLES

Conventional Parameters*		Hydrotreater Feed (%)	Hydrotreater Product (%)	NMR Parameters*		Hydrotreater Feed (%)	Hydrotreater Product (%)
C	(1	88.70±0.13	88.89±0.19		(1	18.01±1.16	12.01±1.06
	(2	88.82±0.28	89.25±0.14	Condensed	(2	12.00±0.76	7.85±0.53
	(3	88.67±0.37	89.08±0.41	Aromatics	(3	26.18±3.59	19.89±4.80
H	(1	7.67±0.07	8.73±0.23		(1	8.26±1.21	6.00±0.57
	(2	8.85±0.25	9.76±0.09	Noncondensed	(2	9.95±1.33	4.87±0.33
	(3	5.69±0.08	6.13±0.25	Aromatics	(3	10.09±1.93	7.34±1.98
N	(1	0.83±0.06	0.70±0.12		(1	17.33±0.76	17.73±0.65
	(2	0.46±0.02	0.29±0.04	Cyclic	(2	13.08±1.64	14.70±1.72
	(3	1.98±0.07	1.68±0.07	Alpha	(3	18.77±1.67	19.76±0.82
S	(1	0.41±0.01	0.18±0.05		(1	9.89±0.71	10.03±0.29
	(2	0.24±0.02	0.03±0.01	Alkyl	(2	10.50±0.60	9.27±0.49
	(3	0.59±0.02	0.49±0.25	Alpha	(3	10.95±0.63	11.03±0.54
O	(1	2.38±0.12	1.51±0.12		(1	13.73±2.48	20.19±0.35
	(2	1.62±0.12	0.67±0.08	Cyclic	(2	16.41±0.75	20.35±1.28
	(3	3.06±0.31	2.63±0.58	beta	(3	13.52±0.71	16.42±1.35
Phenols		1.27±0.30	0.36±0.14		(1	20.61±0.95	21.22±0.66
				Alkyl	(2	22.54±0.70	24.31±0.77
Distillate		56.13±3.53	65.29±4.24	beta	(3	12.86±1.02	13.58±1.56
Nondistillate		43.87±3.53	34.71±4.24		(1	12.17±1.06	12.81±0.43
				Gamma	(2	18.46±2.61	18.64±2.89
Oils		58.28±1.60	75.79±2.90		(3	7.63±0.92	11.98±4.03
Asphaltenes		30.02±1.44	20.42±2.28	Aliphatic	(2	52.81±1.64	64.20±2.16
				Aromatic	(2	33.23±1.55	24.16±1.53
Benzene Insol.		11.70±1.53	3.79±1.10	Aromatic	(2	13.97±1.49	11.64±1.47

*(1) total sample, (2) distillable, and (3) nondistillable fraction.

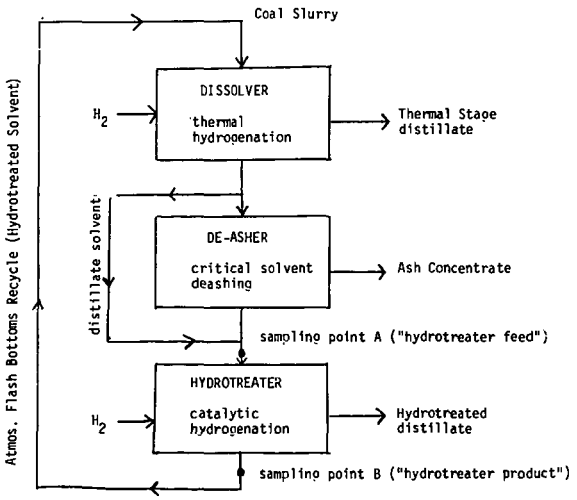

Figure 1. Wilsonville Integrated Two Stage Liquefaction (ITSL) process (simplified scheme).

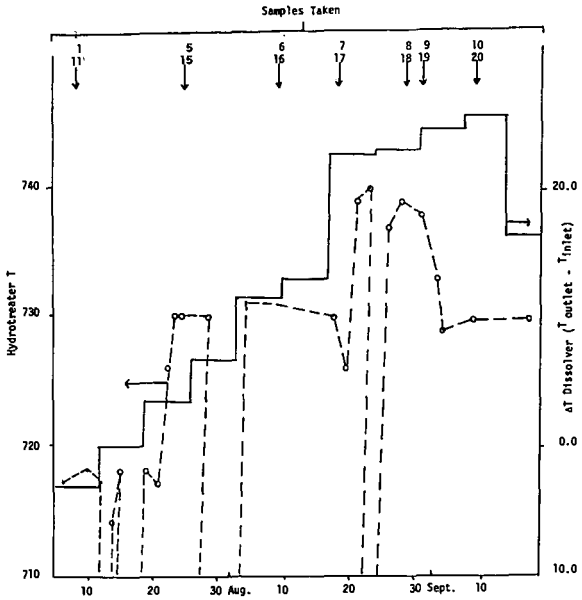

Figure 2. Temperature/-time profile of hydro-treater (--) as well as a seven day average of the difference (Δ T) between the outlet and inlet temperature of dissolver (__) and days on which samples were collected.

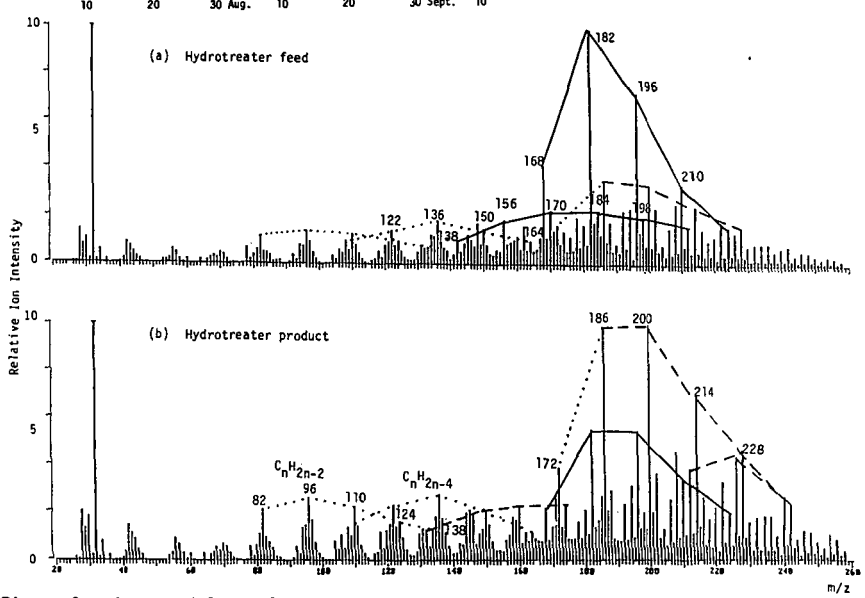

Figure 3. Averaged low voltage mass spectra of the hydrotreater feed (a) and hydrotreater product (flash bottoms) (b).

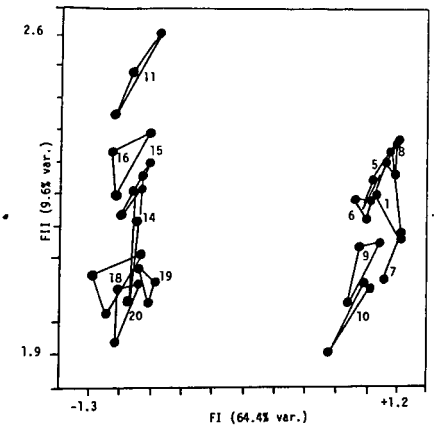

Figure 4. Factor score plot of low voltage MS data in the Factor I and Factor II subspace. Triplicate analyses of the same sample are connected by solid lines. For sample codes see Figure 2.

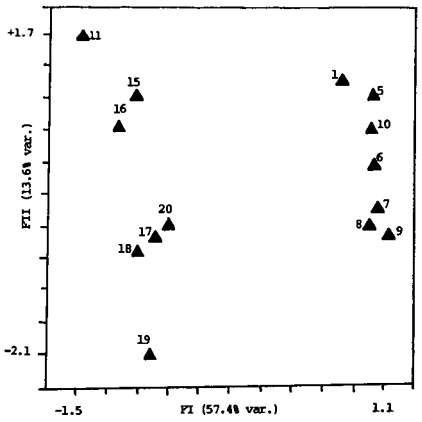

Figure 5. Factor score plot of NMR and conventional data in the Factor I and Factor II subspace, showing two cluster hydrotreater feed (1-10) and hydrotreater product (11-20). For sample codes see Figure 2.

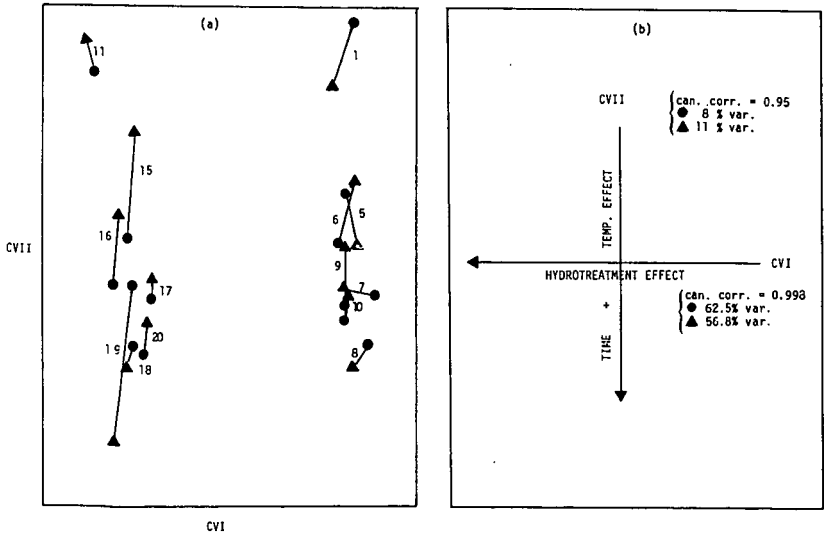

Figure 6. (a) Scores of low voltage MS (●) and scores of NMR and conventional data (▲) in the CVI and CVII subspace. Note the correlation between two data sets. (b) Interpretation of the major trends in the CVI-CVII subspace.

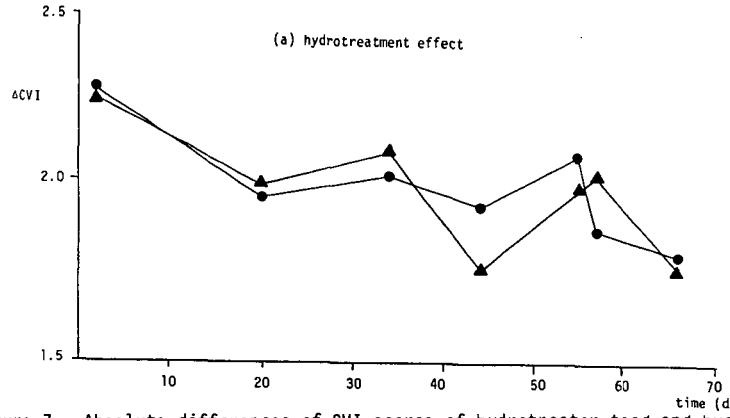

Figure 7. Absolute differences of CVI scores of hydrotreater feed and hydrotreater product for low voltage MS (●) and NMR and conventional data (▲).

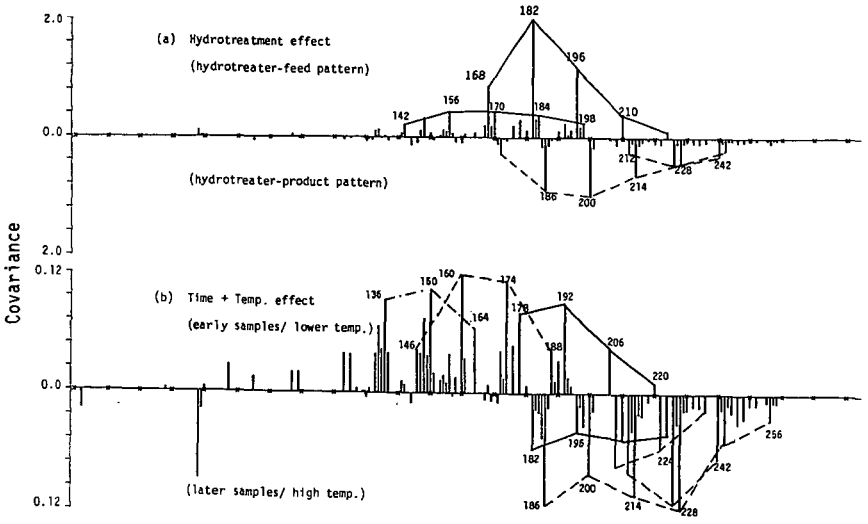

Figure 8. Mathematically extracted spectra of low voltage MS on CVI rotation (a) and CVII rotation (b).

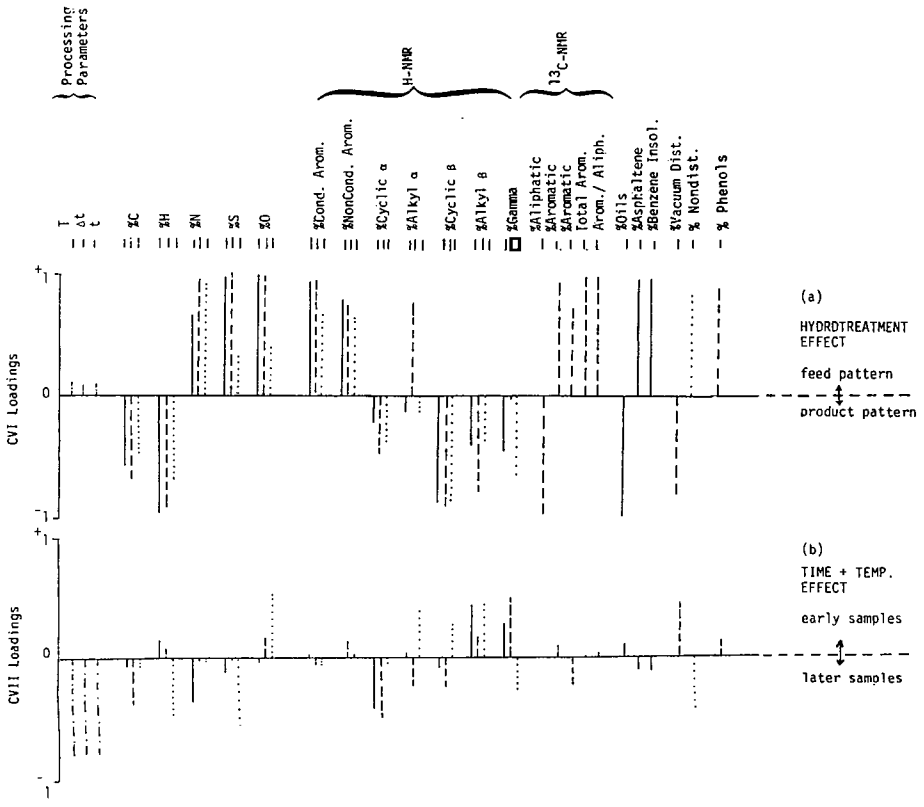

Figure 9. Loading of NMR and conventional variables on CVI (a) and CVII (b). Total sample (-), distillable fraction (--) and nondistillable fraction (...).